Available online at www.sciencedirect.com
SCIENCE DIRECT®
PERGAMON
Chaos, Solitons and Fractals 18 (2003) 593–612
CHAOS SOLITONS & FRACTALS
www.elsevier.com/locate/chaos

The Hicksian floor–roof model for two regions linked by interregional trade

Irina Sushko [a], Tönu Puu [b,*], Laura Gardini [c]

[a] Institute of Mathematics, National Academy of Sciences of Ukraine, Kiev, Ukraine
[b] Center for Regional Science, University of Umeå, Umeå 190187, Sweden
[c] Facoltà di Economia, Università degli Studi di Urbino, Urbino, Italy

Abstract

The Hicksian multiplier–accelerator model with the original floor–roof limits to investments is studied for the case of two regions linked by interregional trade. The result is a piecewise linear continuous four dimensional map, which is reduced to three dimensions through the choice of an appropriate distributed consumption lag. The attractors, basins, and bifurcations of the map are studied under the assumption of a certain symmetry between the regions. The Neimark–Hopf bifurcation for piecewise linear maps is described in detail which gives rise to the appearance of an attracting closed invariant curve homeomorphic to a circle. The structure of resonance regions in the parameter space are investigated.

1. Introduction

1.1. Samuelson's multiplier–accelerator model

There is no doubt that the most used macroeconomic model of business cycles for a period of several decades was due to Paul Samuelson [18], who formalised some ideas by Alvin Hansen in a stringent way. It combined the so called "principle of acceleration" with the "multiplier". The historical roots of the acceleration principle are not quite obvious. It assumed productive capital K to be kept in fixed proportion v to the current production Y, i.e. $K = vY$, as later formalised in the Leontief type of production function where all inputs were limiting. Anyhow, investments I, by definition being the change of capital stock, become proportionate to the change of production volume—or real income, which is the same in macroeconomic terms; this whether the change was measured as a difference in discrete time, i.e. $I_{t+1} = v(Y_t - Y_{t-1})$, or as a time derivative in continuous time. The latter style was mainly employed in growth theory, which we will not consider here, as both Samuelson and, somewhat later, Sir John Hicks in 1950 [9] used a discrete time setting. Noteworthy is, however, that the originator of growth theory, Sir Roy Harrod, in 1950 [8] actually was interested in business cycles, and noted that the balanced growth path he had discovered was unstable. He failed to formulate the second-order process which would have created oscillatory motion even in continuous time. This was left to Goodwin [5] and Phillips [16], but he could hardly be blamed for later growth theorists forgetting about instability.

The multiplier emerged with Keynesian macroeconomics around 1936, and was a fresh new concept by the time Samuelson formulated his model. According to it consumption was proportionate to income, $C_{t+1} = (1 - s)Y_t$, with one constant fraction consumed, and the rest, $S_{t+1} = sY_t$, saved (for ever). Given that in equilibrium income is generated as the sum of consumption and investments, $Y_{t+1} = C_{t+1} + I_{t+1}$, a second-order feed back mechanism was created

* Corresponding author.

0960-0779/03/$ - see front matter © 2003 Elsevier Science Ltd. All rights reserved.
doi:10.1016/S0960-0779(02)00679-3

$$Y_{t+1} = (1 + v - s)Y_t - vY_{t-1}, \tag{1}$$

which is a damped or an explosive oscillator. The name "multiplier" was due to the fact that any fixed initial increment to investments, ΔI, according to the equation $Y_{t+1} = (1 - s)Y_t + \Delta I$, through subsequent spending would give rise to an infinite series of increments to income $\Delta I + (1 - s)\Delta I + (1 - s)^2\Delta I + (1 - s)^3\Delta I + \cdots = \Delta I/s$. As the rate of saving is a fraction, $0 < s < 1$, the multiplier $1/s$ would be a positive number larger than unity, and so an initial investment increase would "multiply" up in its final effect on income.

The same also applies to constant so called "autonomous" expenditures $\mathscr{A}$, for instance government spending, or private investments that are not business cycle dependent. Then the income generation equation changes to $Y_{t+1} = A + C_{t+1} + I_{t+1}$, and the recurrence becomes

$$Y_{t+1} = A + (1 + v - s)Y_t - vY_{t-1}.$$

This new equation obviously has a particular stationary solution $Y_{t+1} = Y_t = Y_{t-1} = A/s$, so, redefining $Y_{t+1} := Y_{t+1} - A/s$, $Y_t := Y_t - A/s$, $Y_{t-1} := Y_{t-1} - A/s$, etc., we regain the original recurrence equation (1). Redefinition of the income variable to its deviation from a positive equilibrium income thus gives sense even to negative values of the variable, at least within certain bounds. Negative values necessarily arise under the iteration of (1). It is noteworthy that the superposition principle still holds under most nonlinearities we may want to introduce.

A final remark to Samuelson's model should be added. In his original contribution, the accelerator was applied to consumption only, not to income. However, the above slight modification, due to Sir John Hicks [9], has become standard in the literature, so we preferred to present it from the outset.

The big problem with the above model is that only in an unlikely borderline case, when $v = 1$, it produces standing oscillations. Otherwise they are damped or explosive. Damping does not really result in a dynamic model, as it only describes the return to eternal equilibrium. Ragnar Frisch in 1933 [3] already suggested that the process be kept going by adding a kind of forcing through random shocks. If so, a model, such as the multiplier–accelerator one, would then provide for some periodicity while in free, though decaying motion. The explosive case by itself is even more absurd than the damped case, as it produces infinite positive and negative values of the variable, and further violates any bounds for the linearisation of smooth but nonlinear functions.

1.2. Hicks's floor and roof model

As a remedy for this Hicks [9] suggested upper and lower limits to the operation of the linear accelerator, which, however, was assumed to be in the explosive range. The reason was not ad hoc, but based on considerations of subject matter facts. An unlimited linear accelerator would in situations of very fast income decrease result in disinvestment which exceed the natural rate of deterioration of the capital stock in the absence of replacement, and so imply active destruction of capital. This does not occur in reality, so there is a lower bound, the "floor", $I_{\min} \leqslant I_{t+1}$ to the acceleration principle $I_{t+1} = v(Y_t - Y_{t-1})$. Likewise, when income increases very fast, scarcities of other inputs than capital (labour or raw materials) become limiting, and there is no point either in pushing investments above an upper bound, the "roof", $I_{t+1} \leqslant I_{\max}$.

The complete Hicksian model hence became nonlinear and, unlike the original Samuelson model, was capable of producing an attractive limit cycle. Suppose we for simplicity assume symmetry for the location of floor and roof. Then, rescaling the variables, we can define the Hicks investment function as

$$H(Y_t - Y_{t-1}) := \begin{cases} (Y_t - Y_{t-1}) & |Y_t - Y_{t-1}| \leqslant 1, \\ \operatorname{sign}(Y_t - Y_{t-1}) & |Y_t - Y_{t-1}| > 1. \end{cases} \tag{2}$$

Accordingly, we have $I_{t+1} = vH(Y_t - Y_{t-1})$, and we can rephrase the iteration (1) as follows:

$$Y_{t+1} = (1 - s)Y_t + vH(Y_t - Y_{t-1}). \tag{3}$$

As already mentioned, on its own, (3) produces an attractive limit cycle provided $v > 1$, otherwise there is only a fixed point at the origin, i.e. no business cycles occur. There is hence the possibility of a Neimark bifurcation of the fixed point.

However, Hicks considered more complicated distributed lag systems, where savings from current income are spent in fractions over several time periods, or equivalently, consumption in any period depends on incomes earned in several previous time periods. Thus the order of the difference equation (3) would increase, and render the possibility of more intricate phenomena of dynamics. The same could be the case with investments. Hommes [10] studied several such interesting cases. In Hicks' days there was, however, no concept of chaos, and no means to analyse these matters, except noting that the result became complicated and messy.

1.3. The open economy for two regions

In what follows, we will complement (3), which is relevant for a closed economy, through interregional trade, and link two oscillators of this type together. In the case of an open economy, the income formation equation is replaced by $Y_{t+1} = C_{t+1} + I_{t+1} + X_{t+1} - M_{t+1}$. To the sum of consumption and investments we add exports and subtract imports. According to a general assumption from the days macroeconomics and business cycle theory arouse, exports to another region were taken proportional to income there, imports proportionate to income in the region itself. This was mainly elaborated by Mezler, in 1950 [13], and earlier publications. Denoting the constant propensity to import by m, and differentiating between the two regions by a suffix, we get $X^1_{t+1} = M^2_{t+1} = mY^2_{t-1}$ and $X^2_{t+1} = M^1_{t+1} = mY^1_{t-1}$, so rephrasing (3), we have

$$\begin{aligned} Y^1_{t+1} &= (1-s_1)Y^1_t + v_1 H(Y^1_t - Y^1_{t-1}) + mY^2_{t-1} - mY^1_{t-1}, \\ Y^2_{t+1} &= (1-s_2)Y^2_t + v_2 H(Y^2_t - Y^2_{t-1}) + mY^1_{t-1} - mY^2_{t-1}. \end{aligned} \tag{4}$$

Taking the same propensity to import m for both regions, we get zero trade balance whenever the two regional incomes are equal. Note that we introduced one extra time period lag for the generation of demand for interregionally traded goods, as compared to that for locally produced goods. Further, in this general statement of (4), we left open the possibility of having different accelerators v_i and saving propensities s_i, but in order to reduce the number of control parameters we later take them equal for both regions.

The system (4) is four-dimensional, and only has one fixed point at the origin of phase space. As processes are difficult to visualize in four dimensions, it is, however, interesting to note that the system can be reduced to three dimensions by a very slight modification.

1.4. Reduction to three dimensions

Instead of assuming that incomes once saved are withdrawn from spending for eternity, let us use the license from Hicks 's original study of distributed lag systems to introduce the simplest lag of all—savings being kept for just one time period, and spent the period after. This was used by one of the authors, see Puu [17], but then in combination with a linear-cubic type of investment function. In the present paper, the original assumptions as to the shape of the investment function (linear with upper and lower bounds) are not modified. By this lagged system there will be contributions to consumption of any period from both two preceding periods, i.e. $C^i_{t+1} = (1-s_i)Y^i_t + s_i Y^i_{t-1}$. The system (4) accordingly changes to

$$\begin{aligned} Y^1_{t+1} &= (1-s_1)Y^1_t + s_1 Y^1_{t-1} + v_1 H(Y^1_t - Y^1_{t-1}) + mY^2_{t-1} - mY^1_{t-1}, \\ Y^2_{t+1} &= (1-s_2)Y^2_t + s_2 Y^2_{t-1} + v_2 H(Y^2_t - Y^2_{t-1}) + mY^1_{t-1} - mY^2_{t-1}, \end{aligned}$$

or, rearranging slightly, to

$$\begin{aligned} (Y^1_{t+1} - Y^1_t) &= v_1 H(Y^1_t - Y^1_{t-1}) - s_1(Y^1_t - Y^1_{t-1}) + m(Y^2_{t-1} - Y^1_{t-1}), \\ (Y^2_{t+1} - Y^2_t) &= v_2 H(Y^2_t - Y^2_{t-1}) - s_2(Y^2_t - Y^2_{t-1}) + m(Y^1_{t-1} - Y^2_{t-1}). \end{aligned}$$

Note that except for the appearance of the last export surplus terms, the processes are autonomous in the income differences $Y^i_{t+1} - Y^i_t$ and $Y^i_t - Y^i_{t-1}$.

It is hence appropriate to introduce new variables for these differences: $U^i_{t+1} := Y^i_{t+1} - Y^i_t$, $U^i_t := Y^i_t - Y^i_{t-1}$. Further, denote income differences between the regions by $Z_t := Y^2_{t-1} - Y^1_{t-1}$. Using these definitions we get

$$\begin{aligned} U^1_{t+1} &= v_1 H(U^1_t) - s_1 U^1_t + mZ_t, \\ U^2_{t+1} &= v_2 H(U^2_t) - s_2 U^2_t + mZ_t. \end{aligned} \tag{5}$$

Observe the opposite signs of the last coupling terms, due to the fact that export surplus for one region is import surplus for the other and vice versa. In order to complete the three dimensional map we just need an updating of the regional income difference equation. We had $Z_t := Y^2_{t-1} - Y^1_{t-1}$, so $Z_{t+1} := Y^2_t - Y^1_t$, and, forming the difference: $Z_{t+1} - Z_t = (Y^2_t - Y^2_{t-1}) - (Y^1_t Y^1_{t-1})U^2_t - U^1_t$. Hence

$$Z_{t+1} = Z_t + U^2_t - U^1_t. \tag{6}$$

The three dimensional map thus becomes

$$T\begin{cases} U_{t+1}^1 = v_1 H(U_t^1) - s_1 U_t^1 + mZ_t, \\ U_{t+1}^2 = v_2 H(U_t^2) - s_2 U_t^2 + mZ_t, \\ Z_{t+1} = Z_t + U_t^2 + U_t^1. \end{cases} \tag{7}$$

This system is autonomous in income differences, two time differences, one for each regional income, and one contemporary income difference between regions. From these differences, incomes, our primary variables of interest, can be obtained as cumulative sums of the first two.

It is interesting to note that for this model we may have more than just one fixed point. The origin still is an obvious candidate, but we can also have two off origin fixed points. Putting $U_{t+1}^i = U_t^i$ and $Z_{t+1} = Z_t$ in (7), we conclude from the last equation that $U_t^1 = U_t^2 = U$, so adding the two first we get $2U = -(s_1 + s_2)U + (v_1 + v_2)H(U)$. Rearranging

$$(2 + s_1 + s_2)U = (v_1 + v_2)H(U).$$

There are now two possibilities for the Hicks function, either $H(U) = U$ or else $H(U) = \pm 1$. In the first alternative $U = 0$ obviously results. However, the second gives us two more alternatives: $U = \pm(v_1 + v_2)/(2 + s_1 + s_2)$. To summarise

$$U = \begin{cases} +\dfrac{v_1 + v_2}{2 + s_1 + s_2}, \\ -\dfrac{0}{2 + s_1 + s_2}. \end{cases}$$

We will later comment on the existence and stability of these three fixed points (see Section 4). The corresponding equilibrium value of $Z_{t+1} = Z_t = Z$ in the fixed points can be calculated from (7), by subtracting the first two equations from which we have $(v_1 - v_2)H(U) + 2Z = 0$. Unless $v_1 = v_2$, we also have $Z = 0$ in the fixed point at the origin. In the off zero cases, we get

$$Z = \frac{v_1^2 - v_2^2}{2m(2 + s_1 + s_2)}$$

for both. Off zero equilibrium thus implies a permanent import surplus for the region with the higher accelerator. If the accelerators are equal, then the export/import surplus is zero in these fixed points as well. Further, due to the fact that the U_t^i variables are defined as income differences, their fixed points mean linear growth or decline, in both regions alike, and at the same constant rate.

1.5. Introduction of further symmetry for the two regions

For the sake of reducing the number of parameters in the model, we already assumed some symmetry. For instance we assumed the propensities to import to be equal for both regions. Further, in the definition of the Hicksian investment function in Eq. (2), it was assumed that the shape of the function, apart from possibly different multiplicative constants v_i, would be perfectly (anti)symmetric, i.e. $I_{\min} = -I_{\max}$.

We could in principle assume much less of symmetric/antisymmetric elements in the model. However, we already have five free parameters to vary. Economists often have the habit of introducing as many different parameters as possible, to the end of achieving some spurious generality or realism. They tend to forget that new parameters in models of given dimension far from always generalise these in terms of producing new phenomena, as this is all regulated by the codimensions.

So, we will rather decrease the number of parameters Suppose the accelerators and propensities to save are equal for the two regions, i.e.

$$v_1 = v_2 \stackrel{\text{def}}{=} v, \quad s_1 = s_2 \stackrel{\text{def}}{=} s \tag{8}$$

in (7).

Putting $U_t^1 + U_t^2 = 0$ in (5), and adding the two equations, we get $U_{t+1}^1 + U_{t+1}^2 = 0$, because from (2) we have $H(-U_t^i) = -H(U_t^i)$. To sum up

$$U_t^1 + U_t^2 = 0 \Rightarrow U_{t+1}^1 + U_{t+1}^2 = 0. \tag{9}$$

Hence, given that the incomes of the two regions initially move in opposite phase, they will continue to do so forever. This means that there is an invariant plane for the process, embedded in its three dimensional phase space. Note that the nonzero fixed points lay off this invariant plane.

2. Properties of the map T

For convenience let us change notation in the model as given in (7) to: $U^1 := x$, $U^2 := y$, and $Z := z$. In this paper, we limit our analysis to the symmetric case (8). Thus, we consider a family of three-dimensional piecewise linear continuous maps $T : \mathbb{R}^3 \to \mathbb{R}^3$ given by

$$T : \begin{pmatrix} x \\ y \\ z \end{pmatrix} \mapsto \begin{pmatrix} vH(x) - sx + mz \\ vH(y) - sy - mz \\ z + y - x \end{pmatrix}, \tag{10}$$

where the function H has the form

$$H(x) = \begin{cases} x, & |x| \leqslant 1, \\ \operatorname{sign}(x), & |x| > 1. \end{cases} \tag{11}$$

The system depends on three real parameters v, s, m. From Section 1, we know that the *feasible* parameter range is

$$v > 0, \quad 0 < s < 1, \quad 0 < m < (1 - s). \tag{12}$$

It is easy to derive the following properties of the map T:

Property 1. *The map T is symmetric with respect to the origin.*

As $T(-x, -y, -z) = -T(x, y, z)$, an important corollary of the Property 1 is the following.

Corollary 1. *A T-invariant set $\mathscr{A}$ is either symmetric with respect to the origin, or there exists one more invariant set symmetric to $\mathscr{A}$ with respect to the origin.*

Property 2. *The plane $x = -y$ is T-invariant, and the restriction of the map T to this plane is a two-dimensional piecewise linear continuous map $F : \mathbb{R}^2 \to \mathbb{R}^2$, given by*

$$F : \begin{pmatrix} y \\ z \end{pmatrix} \mapsto \begin{pmatrix} vH(y) - sy - mz \\ 2y + z \end{pmatrix}. \tag{13}$$

Obviously, the map F too is symmetric with respect to the origin.

From $T(x, x, 0) = T(f(x), f(x), 0)$, where

$$f(x) \stackrel{\text{def}}{=} vH(x) - sx, \tag{14}$$

we immediately have one more property of the map T:

Property 3. *The line $\{x = y, z0\}$ is T-invariant and the restriction of the map T on this line is a one-dimensional map $f : \mathbb{R} > \mathbb{R}$ given by $x \mapsto f(x)$ where the function $f(x)$ is defined in* (14).

Clearly, the map f too is symmetric with respect to the origin. It has rather simple dynamics which is described in Section 4.

In the next section, we describe the dynamic properties of the map F given in (13). In particular, we show that the map F can have periodic, quasiperiodic or chaotic attractors depending on the parameter values. We mainly focus on the Neimark–Hopf bifurcation of the fixed point, which has not yet been completely described for piecewise linear systems. We show that this bifurcation results in an attracting closed invariant curve, which is a piecewise linear set in the case of a rational rotation number, and a smooth curve if the rotation number is irrational. We describe the structure of so-called *resonance regions* in the parameter space, and some bifurcations associated with crossing these regions, which differ from the Arnol'd tongues, well-studied for smooth systems (see, e.g., [1,2]).

In Section 4, we give conditions for the invariant plane $x = -y$ to be globally attracting and analyse the dynamic behavior of the map T.

3. Attractors and bifurcations of the map F

Consider the map F of the form (13). The map F is given by three linear maps denoted F_i, $i = 1, 2, 3$, which are defined, respectively, in the regions R_i

$$F_1 : \begin{pmatrix} y \\ z \end{pmatrix} \mapsto \begin{pmatrix} -v - sy - mz \\ 2y + z \end{pmatrix}, \quad R_1 = \{(y,z) : y < -1, z \in \mathbb{R}\};$$

$$F_2 : \begin{pmatrix} y \\ z \end{pmatrix} \mapsto \begin{pmatrix} (v-s)y - mz \\ 2y + z \end{pmatrix}, \quad R_2 = \{(y,z) : |y| \leqslant -1, z \in \mathbb{R}\};$$

$$F_3 : \begin{pmatrix} y \\ z \end{pmatrix} \mapsto \begin{pmatrix} v - sy - mz \\ 2y + z \end{pmatrix}, \quad R_3 = \{(y,z) : y > 1, z \in \mathbb{R}\}.$$

F is not differentiable on two straight lines $y = -1$ and $y = 1$ which we shall call critical lines LC_{-1} and LC'_{-1}, respectively, following the pioneering work by Gumowski and Mira [7,14]. The critical lines LC_0, LC'_0 are defined as images of LC'_{-1}

$$\{LC_0, LC'_0\} = \{(y,z) : z = -y/m \pm (v - s + 2m)/m, z \in \mathbb{R}\}.$$

The critical line $LC_k(LC'_k)$ of rank $k, k = 1, 2, \ldots$, is obtained as $LC_k = F(LC_{k-1})(LC'_k = F(LC'_{k-1}))$. It is a broken line (i.e. a curve made up of segments of straight lines).

Property 4. *The map F is invertible if $m > s/2$, noninvertible if $m < s/2$.*

To show this, we first note that the strip R_2 always maps into the strip between LC'_0 and LC_0 (see Fig. 1). Then, for $m = s/2$, the half-plane $R_1(R_3)$ maps into the straight line $LC'_0(LC_0)$. Thus, the map F is not uniquely invertible on these two lines. For $m > s/2$, the half-plane $R_1(R_3)$ maps into the half plane below LC'_0 (above LC_0), so that the map is uniquely invertible, while, for $m < s/2$, the half-plane $R_1(R_3)$ maps above LC'_0 (below LC_0). Thus, for $m < s/2$, any point of the strip, bounded by LC'_0 and LC_0, has three distinct rank-1 preimages, one in each of the regions R_1, R_2 and R_3, while any point outside this strip has only one rank-1 preimage, i.e. the map F is noninvertible of so-called $Z_1 - Z_3 - Z_1$ type.

The *fixed points* of the maps $F_1$and F_3 are $(0, -v/m)$ and $(0, v/m)$, respectively. They always belong to the region R_2, where the map F_2 is defined, i.e. they are always outside the definition regions for F_1 and F_3. Thus, the only fixed point of the map F is the fixed point $(0,0)$ of the map F_2.

Proposition 1. *The only fixed point of the map F, given in* (13), *is* $(0,0)$, *and it is attracting iff*

$$(s,m) \in S \stackrel{\text{def}}{=} \{(s,m) : s - 1 - v < m < (1 + s - v)/2, m > 0\} \tag{15}$$

for any fixed $v > 0$.

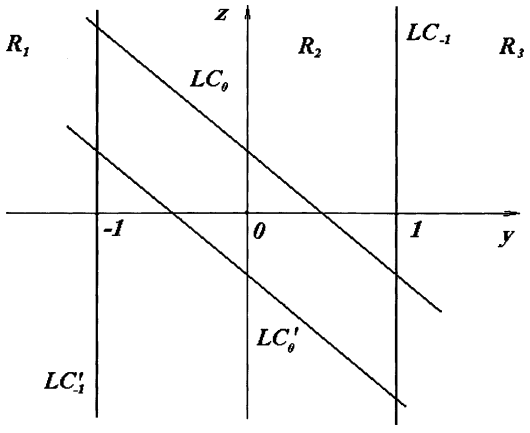

Fig. 1. Critical lines of the map F.

The eigenvalues $\lambda_{1,2}$ of the Jacobian matrix DF_2 are

$$\lambda_{1,2} = \left(1 + v - s \pm \sqrt{(1 - v + s)^2 - 8m}\right) \Big/ 2, \tag{16}$$

which are real for $m \leqslant (1 - v + s)^2/8$ and complex for $m > (1v + s)^2/8$. To show that the proposition holds, recall that for a linear map L, its fixed point is attracting iff the eigenvalues of DL are less then 1 in modulus. The necessary and sufficient conditions for this are the following

$$\begin{cases} 1 + \det DL + trDL > 0, \\ 1 + \det DL - trDL > 0, \\ 1 - \det DL > 0. \end{cases}$$

For the map F_2 the above inequalities define, after some algebra, the triangle S given in (15).

Note that depending on the parameters the stability triangle S may have no intersection with the feasible parameter range (12). Taking into account this range, we show schematically in Fig. 2 the stability (instability) conditions for the fixed point $(0, 0)$ in the (s, m)-parameter plane for different values of v. It can be seen that the stability region of the fixed point in the feasible region decreases as the value of v increases: for $v > 2$ the fixed point $(0, 0)$ is always unstable in the feasible triangle.

The maps F_1 and F_3 only differ by shift constants $(\pm v >, 0)$. Thus they have qualitatively similar dynamics. The eigenvalues of the Jacobian matrix $DF_1 = DF_3$ are

$$\mu_{1,2} = (1 - s \pm \sqrt{(s + 1)^2 - 8m})/2, \tag{17}$$

which are real if $m < (s + 1)^2/8$, and complex if $m > (s + 1)^2/8$. In the (s, m)-parameter plane the triangle S_1, given by

$$S_1 \stackrel{\text{def}}{=} \{(s, m) : s - 1 < m < (1 + s)/2, m > 0\} \tag{18}$$

is such that if $(s, m) \in S_1$ then $|\mu_{1,2}| < 1$.

Proposition 2. *For $m > (1 + s)/2$ almost all the trajectories of the map F are diverging.*

To see this, note that $|\mu_{1,2} > 1$ for $m > (1 + s)/2$, i.e. the maps F_1 and F_3 are expanding. Obviously, the condition $m > (1 + s - v)/2$ also holds, thus $|\lambda_{1,2}| > 1$, i.e. the map F_2 is expanding as well. Due to invertibility of the map F for the parameter range considered, we can state that the map T^k is expanding for any $k > 0$. Thus, no stable cycle can exist for F, but some unstable cycles, for example, the fixed point $(0, 0)$. Moreover, considering the images of the critical curves, no absorbing area can be obtained. Therefore, almost all the trajectories are diverging.

It is worth to note that crossing the stability region through different edges of the triangle S, different bifurcations occur. Crossing the line $m = s - 1 - v$ (at which one eigenvalue is equal to -1) we have a *flip bifurcation* which for

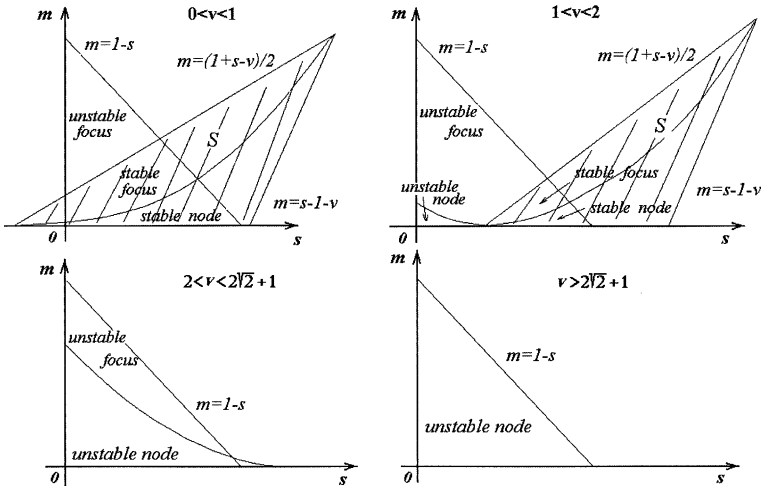

Fig. 2. The stability (instability) regions for the fixed point $(0, 0)$ in the (s, m)-parameter plane for different ranges of v.

piecewise linear maps is not associated with a period-doubling phenomena (see, e.g., [12]). Crossing the line $m = 0$ one eigenvalue crosses the value $+1$, and the fixed point becomes a saddle. However these bifurcation curves are outside the feasible region and we do not comment them here. The only bifurcation we are interested in is the one occurring for

$$m^* \stackrel{\text{def}}{=} m = (1 + s - v)/2, \tag{19}$$

when the fixed point becomes a center. After the bifurcation the fixed point becomes a repelling focus. Thus we have a piecewise linear analogue of the Neimark–Hopf bifurcation for smooth maps [11].

In order to get a general view of the dynamics of F, we show here some two-dimensional bifurcation diagrams in the (s, m)-parameter plane for fixed values of v. Let $P_{l/k}$ denote a region in the (s, m)-parameter plane, such that for $(s, m) \in P_{l/k}$ the map F has an attracting cycle of period k with rotation number l/k, where l/k is an irreducible fraction. The resonance regions $P_{l/k}$ are shown by different colors for $k \leqslant 34$, $v = 0.9$ (Fig. 3) and $v = 1.7$ (Fig. 4). Note that, even

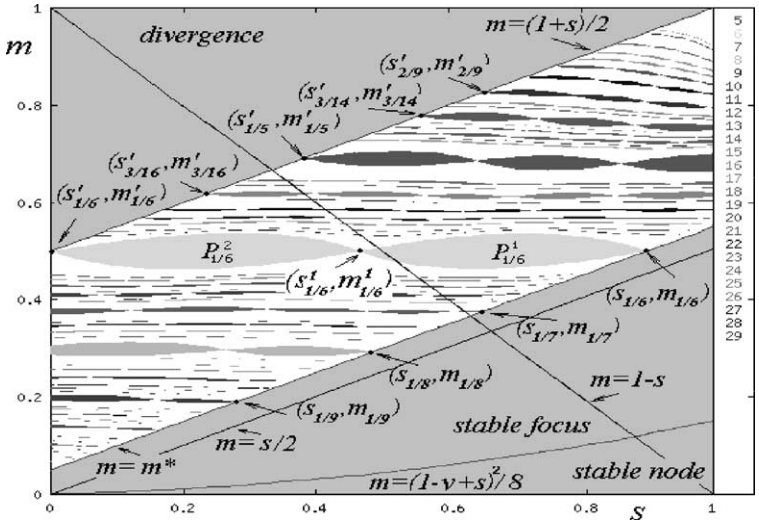

Fig. 3. Two-dimensional bifurcation diagram for the map F in the (s, m)-parameter plane for fixed $v = 0.9$. The resonance regions $P_{l/k}$ are shown by different colors.

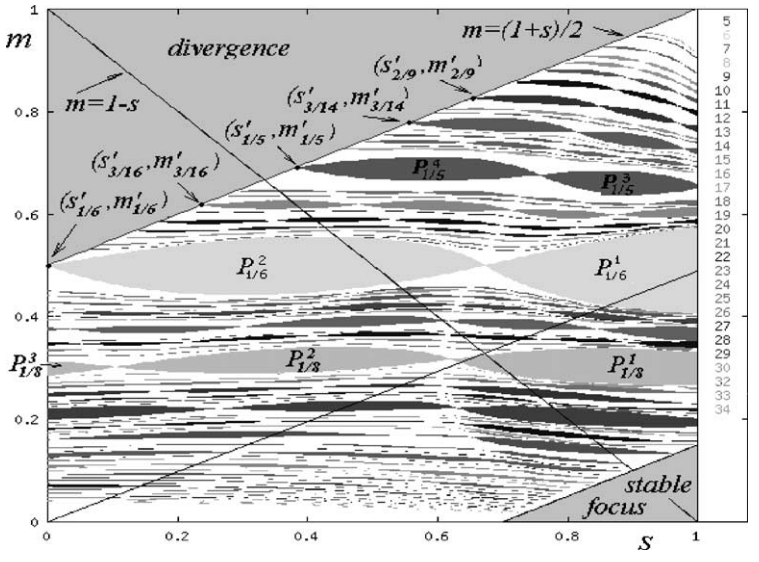

Fig. 4. Two-dimensional bifurcation diagram for the map F in the (s, m)-parameter plane at $v = 1.7$.

if the feasible parameter range is $m < (1 - s)$, we present a wider parameter window. The white regions in these diagrams correspond to attracting cycles of periods $k > 34$, or quasi-periodic behavior, or chaotic attractors.

3.1. Periodic and quasiperiodic attractors. Description of the resonance regions

Let $v = 0.9$ (see Fig. 3). If the (s, m)-parameter point crosses the straight line $m = m^*$ (19) then the fixed point $(0, 0)$ (which is an attracting focus for $m < m^*$) loses stability with a complex pair of eigenvalues for DF_2. As we shall see, in similarity to the Neimark–Hopf bifurcation for smooth nonlinear systems [6], the result of this bifurcation is the appearance of an attracting closed invariant curve $\mathscr{A}$, homeomorphic to a circle. This set does not appear in a neighborhood of the fixed point, as it does for smooth maps, but far from the fixed point: its position depends on the critical lines of the map.

Similarly to the rotation numbers for the circle maps, we can use a rotation number for the map F: it can be rational l/k, or irrational, being the average rotation of any initial point on $\mathscr{A}$ around the repelling fixed point $(0, 0)$. The value l/k depends on the parameters.

In the case of a rational rotation number l/k, with k even, an attracting and a saddle cycle of period k, denoted $\gamma_{l/k}$ and $\gamma'_{l/k}$, respectively, exist on $\mathscr{A}$, which in this case is made up by the unstable set of the period-k saddle cycle $\gamma'_{l/k}$. The unstable set of $\gamma'_{l/k}$, consists of linear segments approaching the points of the attracting period-k cycle $\gamma_{1/k}$. An example is presented in Fig. 5 where the cycles $\gamma_{1/8}$ and $\gamma'_{1/8}$ are shown together with the unstable set of $\gamma'_{1/8}$ for $s = 0.4$, $m = 0.3$. The attracting closed invariant curve $\mathscr{A}$, associated with parameter values belonging to some resonance region, is called a "saddle-connection". As we will show later (see Proposition 7), contrary to what occurs in smooth maps, this set is piecewise-linear, with a countable number of kink points.

Due to the necessary asymmetry with respect to the origin for any cycle of odd period k, there must exist on $\mathscr{A}$ one more cycle of the same period, so that they together provide for the symmetry (see corollary 1). Thus, for k odd, there are two coexisting attracting cycles $\gamma^1_{l/k}$ and $\gamma^2_{l/k}$ on $\mathscr{A}$ and two saddle cycles $\gamma'^1_{l/k}$ and $\gamma'^2_{l/k}$ of period k. (Below, we omit the suffix if the statement holds for both cycles). In this case, the closed invariant curve $\mathscr{A}$ still is homeomorphic to a circle. It is made up by the unstable sets of two saddle cycles, and consists of linear segments approaching the points of the attracting cycles. Thus it is still a saddle-connection, and $\mathscr{A}$ is a piecewise-linear set. Fig. 6 shows an example of the attracting cycles $\gamma^1_{1/7}$ and $\gamma^2_{1/7}$ with their basins of attraction and the saddle cycles $\gamma'^1_{1/7}$ and $\gamma'^2_{1/7}$ with their unstable sets which form the curve $\mathscr{A}$.

We also note that in Figs. 5 and 6 the attracting cycles are nodes. However, they may also be attracting foci. The only difference in this case is that the invariant curve $\mathscr{A}$ (always made up by the unstable sets of the saddles) consists of linear segments, which approach the points of the period-k; focus and spiral around them.

In Fig. 3 a particular "sausage" structure of $P_{l/k}$ can be seen, which may be explained as follows: each subregion of $P_{l/k}$ corresponds to a certain combination of the maps F_1, F_2 and F_3, which have to be applied in order to get all the points of the cycle $\gamma_{l/k}$, and this combination is different in each subregion of $P_{l/k}$. For instance, there are two subregions of $P_{1/6}$, denoted $P^1_{1/6}$ and $P^2_{1/6}$ in Fig. 3. Let $(y_0, z_0) \in R_3$, be a point of $\gamma_{1/6}$. Then $(y_0, z_0) = F^6(y_0, z_0)$, and for the cycle $\gamma_{1/6}$ which exists at $\gamma_{1/6}$ which exists at $(s, m) \in P^1_{1/6}$, we have

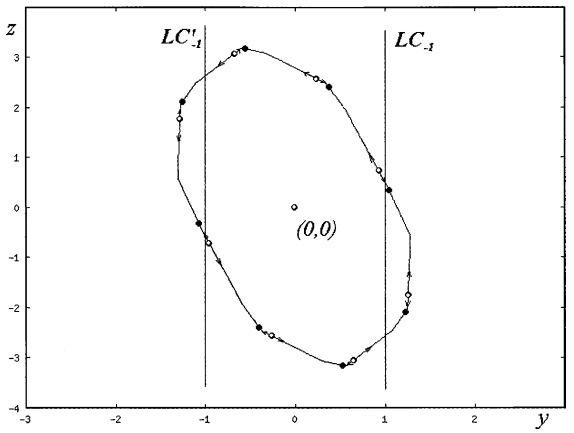

Fig. 5. An attracting closed invariant curve $\mathscr{A}$ made up by the unstable set of the saddle cycle $\gamma'_{1/8}$ approaching the points of the attracting cycle $\gamma_{1/k}$ ($v = 0.9$, $s = 0.4$, $m = 0.3$).

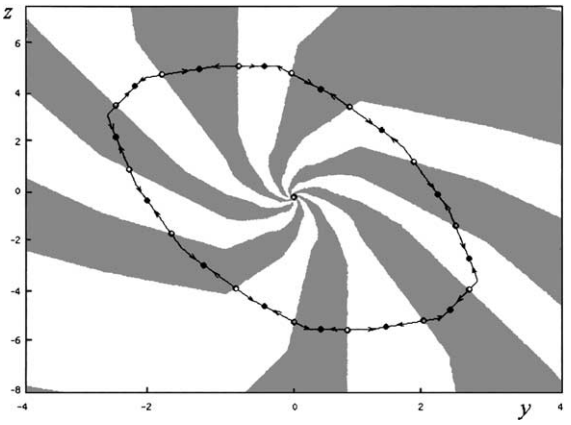

Fig. 6. The attracting cycle $\gamma^1_{1/7}$ and $\gamma^2_{1/7}$ with their basins of attraction and the saddle cycles $\gamma'^1_{1/7}$ and $\gamma'^2_{1/7}$ with their unstable sets which form the invariant curve $\mathscr{A}$ ($v = 0.9$, $s = 0.2$, $m = 0.38$).

$$F^6 = F_3 \circ F_2 \circ F_1 \circ F_1 \circ F_2 \circ F_3$$

(the rotation is in the counter-clockwise direction). Note that any cyclical composition of the maps given above works, i.e., we may equivalently write $F^6 = F_2 \circ F_1 \circ F_1 \circ F_2 \circ F_3 \circ F_3$, or $F^6 = F_1 \circ F_1 \circ F_2 \circ F_3 \circ F_3 \circ F_2$ and so forth.

If $(s, m) \in P^2_{1/6}$, then we have a different composition of the maps:

$$F'^6 = F_3 \circ F_1 \circ F_1 \circ F_1 \circ F_3 \circ F_3.$$

Also note that in F^6 and F'^6, we have given the compositions associated with the attracting cycle $\gamma_{1/6}$ of the map F, and that a different composition of the maps is associated with the saddle cycles $\gamma'_{1/6}$ which give the saddle connection $\mathscr{A}$.

A natural question arises looking at Figs. 3 and 4: which curves form the boundaries of the resonance regions? We know that for smooth systems the boundaries of Arnol'd tongues are formed by curves corresponding to saddle-node bifurcation. The same occurs in piecewise linear maps, but the bifurcation value is not characterised as in smooth maps. For piecewise linear (or piesewise smooth) systems, the main role is played by a *border-collision bifurcation* which occurs when a cycle belongs to the line of nondifferentiability of the map, i.e., the critical lines (see [14,15]). For the map considered, if the (s, m)-parameter point crosses the boundary of $P_{l/k}$ transversally, then, in the case of an even k, one point of the attracting cycle $\gamma_{l/k}$ belongs to LC_{-1} and the point of $\gamma_{l/k}$, symmetric to it with respect to the origin, belongs to LC'_{-1}. For an odd k, one point of $\gamma^1_{l/k}$ belongs to LC_{-1}, and one point of $\gamma^2_{l/k}$ belongs to LC'_{-1}. At this border-collision bifurcation a saddle-node, or a saddle-focus bifurcation also occurs, involving the saddle cycle $\gamma'_{l/k}$, whose unstable set provides the invariant curve $\mathscr{A}$. Note that, for piecewise linear maps, the saddle-node bifurcation may occur only when points of both the attracting and saddle cycles are located on the critical lines. In Fig. 7 we show the one-dimensional bifurcation diagram, associated with the crossing of the resonance region $P^2_{1/6}$ for $s = 0.2$, $m \in [0.45, 0.55]$. In this diagram the m values are displayed on the horizontal axis while the vertical axis shows the projection of a typical (y, z)-trajectory on the y-axis.

We can obtain the parameter values $(s_{l/k}, m_{l/k})$, corresponding to the bifurcation of the fixed point $(0, 0)$ resulting in the appearance of the cycles $\gamma_{l/k}$ and $\gamma'_{l/k}$ which form the closed invariant curve $\mathscr{A}$. At the bifurcation value the expression for $\lambda_{1,2}$ can be written as $\lambda_{1,2} = \mathrm{Re}\lambda_{1,2} \pm i\mathrm{Im}\lambda_{1,2}$, where $\mathrm{Re}\lambda_{1,2} = \cos 2\pi l/k$. From (16) and (19) we have

$$s_{l/k} = 1 + v - 2\cos 2\pi l/k,$$
$$m_{l/k} = 1 - \cos 2\pi l/k.$$

For example, for the resonance region $P_{1/5}$ we get $S_{1/5} \approx 1.282$, $m_{1/5} \approx 0.691$; for $P_{1/6}$ these values are $s_{1/6} = v$, $m_{1/6} = 0.5$; for $P_{1/8}$ we have $s_{1/8} = 1.9 - \sqrt{2}$ and $m_{1/8} = 1 - \sqrt{2}/2$, and so on (see Fig. 3). The following proposition describes the dynamic behaviour of the map F at the bifurcation values $s = s_{l/k}$, $m = m_{l/k}$.

Proposition 3. *Let $s = s_{l/k}$, $m = m_{l/k}$. Then in the phase space there exists an invariant attracting polygon Π. The edges of Π are k segments of the critical lines LC_i and LC'_i, $i = -1, \ldots, k/2 - 1$, for even k; and $2k$ segments of LC_j and LC'_j,*

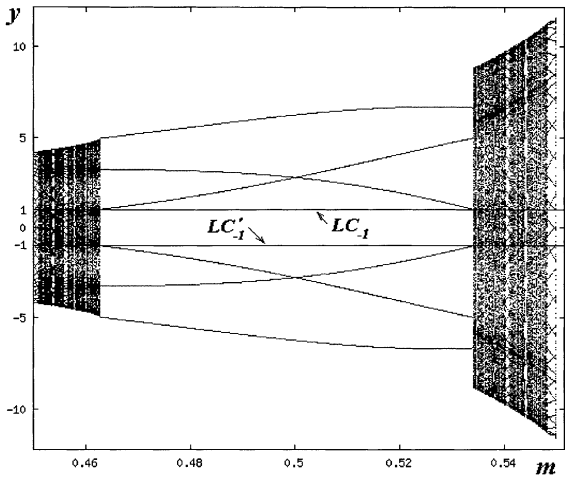

Fig. 7. One-dimensional bifurcation diagram associated with the crossing of the resonance region $P^2_{1/6}$ for $v = 0.9$, $s = 0.2$ and $m \in [0.45, 0.55]$.

$j = -1, \ldots, k-1$, *for odd* k. *Any point* $(y_0, z_0) \notin \Pi$ *is* k*-periodic*; *any point* $(y_0, z_0) \notin \Pi$ *is attracted to a period-*k *cycle on the boundary of* Π.

To show this, let us first consider the case $l/k = 1/6$, that is we fix $s = s_{1/6}$, $m = m_{1/6}$. Then the eigenvalues of F_2 are complex-conjugate with $|\lambda_{1,2}| = 1$, thus, the fixed point $(0, 0)$ is a center. Let us construct an invariant set which exists in this case. First of all, it must include all the invariant curves (ellipses) of the map F_2 in R_2 (see Fig. 8). Each point of these ellipses is periodic with the rotation number 1/6. This invariant set must also include all the six cycles of F_2 belonging to the invariant curves of F_2 which cross the critical lines LC_{-1} and LC'_{-1} but such that the periodic points are all included in the closure of R_2. This gives rise to a polygon Π with six edges, tangent to the ellipse of F_2, itself tangent to LC_{-1} and LC'_{-1}.

Thus there exists a polygon Π in the phase space, such that any point belonging to the interior of Π, or to the edges of Π is six-periodic, and its images rotate around the origin (a centre) with rotation number 1/6. Due to the invertibility of the map F for the parameter range considered, only the boundary of Π is an attracting set, because no point of the phase plane can be mapped in the interior of Π. Any initial point outside Π is attracted to a period-6 cycle, belonging to the boundary of Π. The edges of the polygon Π are segments of critical lines LC_i and LC'_i for $i = -1, 0, 1$, with vertices a_i and a'_i, where $a_{-1} = LC_{-1} \cap LC_0$, $a'_{-1} = LC'_{-1} \cap LC'_0$, $a_i = F(a_{i-1})$, $a'_i = F(a'_{-i})$. Note that the points a_i and a'_i are also six-periodic. Only the map F_2 is applied in order to get all the points of the cycles of period 6.

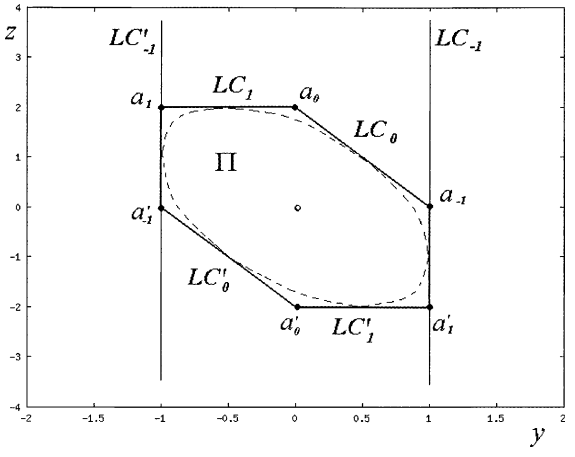

Fig. 8. An attracting invariant polygon Π at bifurcation values $v = 0.9$, $s = 0.9$ and $m = 0.5$.

Similar considerations can be provided for any value $1/k$ with even k. As for k odd, the only difference is that the polygon Π in this case is made up by $2k$ segments of critical lines, corresponding to the pair of coexisting cycles of odd period k, and the total number of periodic points to take in account is $2k$; instead of k.

Proposition 4. *The number n of subregions of the resonance region $P_{l/k}$ is equal to $n = k/2 - 1$ for k even, and to $n = k - 1$ for k odd.*

Let k be even. Consider again the case $l/k = 1/6$. Let $(s^1_{1/6}, m^1_{1/6})$ denote the transition point from the subregion $P^1_{1/6}$ to the subregion $P^2_{1/6}$ (see Fig. 3). What occurs at the crossing through the point $(s^1_{1/6}, m^1_{1/6})$ is shown in the one-dimensional bifurcation diagram in Fig. 9. The horizontal axis represents values of the parameter $s \in [0.4 : 0.5]$ and the vertical shows projections of the points of $\gamma_{1/6}$ (red lines) and of $\gamma'_{1/6}$ (blue lines) to the y-axis, $m = 0.5$. This one-dimensional bifurcation diagram puts in evidence that, as long as the parameter point $(s, m) \in P^1_{1/6}$, the map F has the attracting six-cycle $\gamma_{1/6}$ with two points in each region R_i, $i = \overline{1,3}$, (due to the symmetry of the cycle with respect to the y-axis, we only see three branches). There also exists a saddle cycle $\gamma'_{1/6}$, such that four points of it are in R_2 (we see only two branches), one point in R_1 and one in R_3.

At the point $(s^1_{1/6}, m^1_{1/6})$ a border-collision bifurcation related to a particular *transcritical bifurcation*, or *exchange of stability* between $\gamma_{1/6}$ and $\gamma'_{1/6}$, occurs (it is particular because at the bifurcation value the cycles are not merging, as it occurs in smooth maps, and the periodic points are critical points). After the bifurcation, when $(s, m) \in P^2_{1/6}$, the former saddle cycle $\gamma'_{1/6}$, becomes attracting, we rename this cycle $\gamma_{1/6}$, with three points in R_1 (on the projection we see only two branches) and three in R_3 (again, we see only two branches). The former attracting cycle $\gamma_{1/6}$ becomes a saddle, so we rename it $\gamma'_{1/6}$, with two points in each region R_i (on the projection we see only one point in each region).

Similar border-collision bifurcations occur when "waist" points in other resonance regions are crossed. The rightmost subregion of $P_{l/k}$, with k even, is such that $k - 4$ points of $\gamma_{l/k}$ are in R_2, two in R_1 and two in R_3. After each subsequent transition of the (s, m)-parameter point from the subregion $P^i_{l/k}$ to $P^{i+1}_{l/k}$, both attracting and saddle cycles have two points less in R_2. After the transition to the leftmost subregion of $P_{l/k}$ the map F has zero points of $\gamma_{l/k}$ in R_2, and two points of $\gamma'_{l/k}$ in R_2. Thus, the number n can be obtained from the equation $k - 4 - 2(n - 1) = 0$ (or $k - 2 - 2(n - 1) = 2$, which is the same).

For odd k the only difference is that the total number of periodic points to take into account is $2k$ instead of k.

From the arguments given above we can see that the following proposition is also true.

Proposition 5. *The leftmost subregion of the resonance region $P_{l/k}$ in the (s, m)-parameter bifurcation diagram of the map F corresponds to a composition of the maps F_1 and F_3 only.*

We can obtain the parameter values $(s'_{l/k}, m'_{l/k})$, corresponding to the contact of $P_{l/k}$ with the straight line $m = (1 + s)/2$ of divergence to infinity. Suppose the (s, m)-parameter point crosses this line from the left to the right,

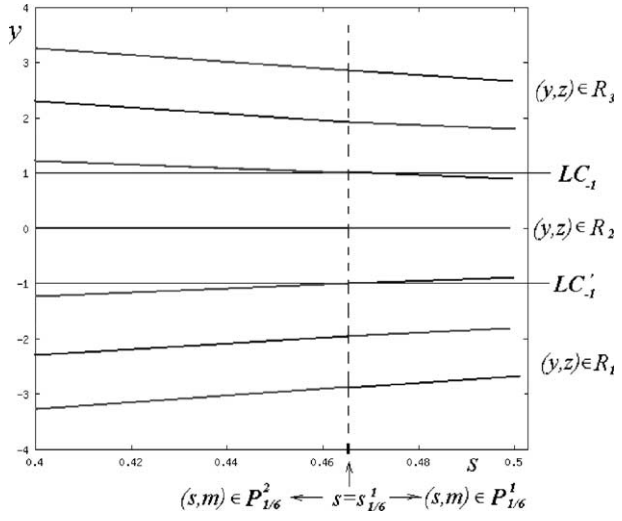

Fig. 9. One-dimensional bifurcation diagram of the map F at $m = 0.5$, $u = 0.9$ and $s \in [0.4, 0.5]$.

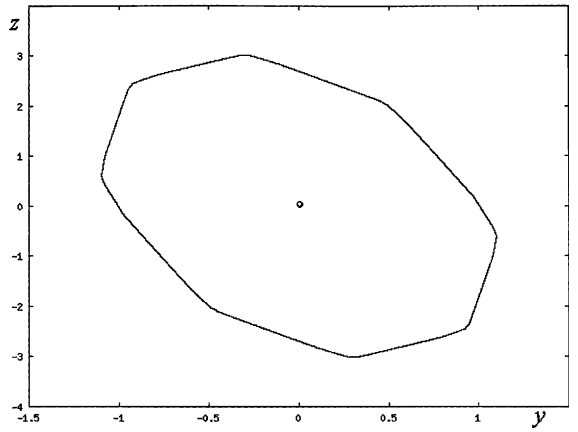

Fig. 10. An example of $\mathscr{A}$ with quasiperiodic, or periodic with very high period, trajectory at $v = 0.9$, $s = 0.4$ and $m = 0.26$.

and enters the region $P_{l/k}$. According to Proposition 5 only the maps F_1 and F_3 need be applied in order to get all the points of the cycle $\gamma_{l/k}$. At $m = (1+s)/2$ the eigenvalues $\mu_{1,2}$ of the linear maps $F_{1,2}$ are complex-conjugate with $|\mu_{1,2}| = 1$, thus the fixed points (foci) of F_1 and F_3 become attracting. Any initial point from R_1 or R_3 begins a rotation around these fixed points while any initial point from R_2 leaves this region in a finite number of iterations (because F_2 is expanding). On the bifurcation line $m = (1+s)/2$ we get exactly a period-k rotation with rotation number l/k if

$$\mathrm{Re}\mu_{1,2} = \cos 2\pi l/k.$$

Thus, using (17), we get

$$s'_{l/k} = 1 - 2\cos 2\pi l/k,$$
$$m'_{l/k} = (1 + s_{l/k})/2 = 1 - \cos 2\pi l/k = m_{l/k}.$$

For example, for the resonance region $P_{1/5}$ we get $m'_{1/5} \approx 0.691$ and $s'_{1/5} \approx 0.382$. For $P_{1/6}$ these values are $m'_{1/6} = 0.5$ and $s'_{1/6} = 0$. For $P_{1/8}$, we have $s'_{1/8} = 1 - \sqrt{2}$ and $m'_{1/8} = 1 - \sqrt{2}/2$, and so forth (see Fig. 3).

Consider now the case when the rotation number of the map F on the closed invariant curve $\mathscr{A}$ is irrational. In this case the set $\mathscr{A}$ is a smooth curve with a quasiperiodic trajectory on it. Fig. 10 shows an example of $\mathscr{A}$ with quasiperiodic, or periodic with very high period, trajectory for $s = 0.4$, $m = 0.26$.

Proposition 6. *At a bifurcation with irrational rotation number* ($m = (1 - v + s)/2$, $s \neq s_{1/k}$, $m \neq m_{l/k}$), *there exists an invariant attracting set C bounded by an ellipse* $\mathscr{E}$ *such that any point* $(y,z) \notin C$ *has a quasiperiodic trajectory*; *any point* $(y,z) \notin C$ *ultimately will have a quasiperiodic trajectory on* $\mathscr{E}$.

At $m = (1 - v + s)/2$ the eigenvalues of F_2 are complex-conjugate with $|\lambda_{1,2}| = 1$, thus, the fixed point $(0,0)$ is a center. If $s \neq s_{l/k}$, $m \neq m_{l/k}$, i.e., the rotation number is irrational, then the invariant set C is bounded by an invariant curve $\mathscr{E}$ (an ellipse) of F_2, tangent to the critical lines LC_{-1} and LC'_{-1} and filled with other invariant curves (ellipses) of F_2, on which the dynamics are quasiperiodic. In this case all critical lines $LC_i, LC'_i, i \geqslant 0$, are tangent to $\mathscr{E}$. Due to the invertibility of the map, any initial condition $(y,z) \notin C$ has the ellipse $\mathscr{E}$ as an ω-limit set.

As we have seen, Proposition 3 describes the dynamics of the map F when the (s,m)-parameter values belong to the Neimark–Hopf bifurcation curve $m = m^*$ (19) and the rotation number of F_2 is rational. Proposition 6 takes into account the case of irrational rotation numbers. The next proposition describes the structure of the attracting closed invariant curve $\mathscr{A}$ which appears after the bifurcation when $(s,m) \in P_{l/k}$. Recall that the map F is invertible for the parameter range considered.

Proposition 7. *If* $(s,m) \in P_{l/k}$ *and the corresponding saddle cycle* $\gamma'_{l/k}$ *has no homoclinic points*, *then the attracting closed invariant curve* $\mathscr{A}$ *is made up by the unstable set* $\gamma'_{l/k}$ *and consists of infinitely many linear segments approaching the attracting cycle* $\gamma_{l/k}$.

In order to be clearer, we fix $k = 8$, that is, let $(s, m) \in P^1_{1/8}$. Then the map F has the attracting cycle $\gamma_{1/8}$ and the saddle cycle $\gamma'_{1/8}$ which form the attracting closed invariant curve $\mathscr{A}$ (see Fig. 5), whose structure is going to be explained.

The eight iteration of the map F, i.e. the map F^8, has 8 saddles and 8 nodes, denoted S_i and N_i, respectively, $i = 1, \ldots, 8$, which are, obviously, points of the 8-cycle $\gamma_{1/8}$ and $\gamma'_{1/8}$. Note that F^8 is a piecewise linear map defined by several linear maps in different regions of the phase space. These regions are separated by the set $LC_{-1}(F^8)$ of critical lines of the map F^8

$$LC_{-1}(F^8) = \bigcup_{k=1}^{8} LC_{-k}(F); LC_{-k}(F) = F^{-1}(LC_{-k+1}).$$

We also denote

$$LC_0(F^8) = F^8(LC_{-1}(F^8)) = \bigcup_{k=0}^{7} LC_k(F).$$

An enlarged part of the invariant area bounded by $\mathscr{A}$ is shown in Fig. 11 where we have coloured in grey an F^8-invariant area B of phase space. This area is bounded by the left branches of the stable sets of the saddle S_1 and S_2, and by a portion of $\mathscr{A}$ made up by the right branch of the unstable set of S_1 and left branch of the unstable set of S_2, both approaching the node N_1. The assumption that the saddle cycle on $\mathscr{A}$ has no homoclinic points, guarantees that such a set B is invariant.

Consider, for example, the saddle S_1. Let us take a linear segment of the local unstable set of S_1 up to its intersection with $LC_0(F^8)$. Denote this segment of straight line by γ. The whole unstable set to the left of N_1 is made up by the infinitely many images of γ under F^8, i.e. $\cup_{n>0}(F^8)^n(\gamma)$. The first iteration of γ by F^8 includes one kink point. Thus, all consequent iterations of γ, converging to the node N_1, include kink points in a numerable sequence also converging to N_1.

In Fig. 11, we also show another segment η which crosses $LC_{-1}(F^8)$. Its image $F^8(\eta)$ is an arc which clearly includes a kink point. Although the numerical simulations show only a few of such points, they must be infinitely many, approaching the node N_1.

The reasoning used above works well for any parameter values inside other resonant regions $P_{l/k}$. The only difference occurs for odd k, in which case we have to consider the periodic points of two different cycles instead of two periodic points of the same saddle, in order to construct the invariant region B. Moreover, the attracting cycle may be a stable focus instead of a stable node.

Up to now we have considered the fixed value of the parameter v, namely, $v = 0.9$. Our conjecture is that all the propositions in this subsection hold for any $v < 1$, range in which we have not found any complex behaviour. In fact, the simple structure of the (s, m)-bifurcation plane for $v < 1$ suggests that in this case the map F cannot have chaotic attractors. Depending on the parameter values it either has an attracting cycle of even period, or two coexisting attracting cycles of odd period, or an invariant closed attracting curve $\mathscr{A}$ with a quasiperiodic trajectory on it. As

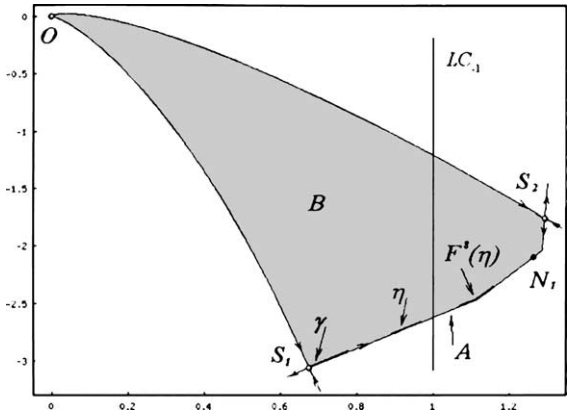

Fig. 11. Portion of the attracting closed invariant curve $\mathscr{A}$ and area B of the phase space which is invariant for F^8.

computer simulations show, for $v > 1$, besides these attractors, the map F may have a chaotic attractor (cyclic or in one piece), and coexistence of different attractors may occur. Some examples are given in the next subsection.

3.2. The routes to complex behavior

Let us now consider the (s, m)-bifurcation diagram of the map F at $v = 1.7$ (Fig. 4). At first sight, it looks similar to Fig. 3, but we can now find parameter values such that the map F has a chaotic attractor.

Consider again the stability loss for the fixed point $(0, 0)$ when the (s, m)-parameter point crosses the bifurcation line $m = m^*$ (19), for instance, at $s = 0.85$, $m = 0.075$. We decrease the value of s: For $s = 0.84$ there exists an attracting invariant closed curve $\mathscr{A}$ shown in Fig. 12. An enlarged part of this attractor is shown in Fig. 13. We can guess that in similarity to the previous consideration, the stability loss of the fixed point can give rise to an attracting closed invariant curve $\mathscr{A}$, homeomorphic to a circle, with periodic or quasiperiodic behavior on it. Note that the map F is noninvertible for $m < s/2$. Thus it is noninvertible at the fixed point bifurcation $m = m^*$.

The resonance regions can be overlapping, which corresponds to coexistence of attracting cycles of different periods. See Fig. 14, where an enlarged part of the phase space is shown at $s = 0.8$, $m = 0.1$ when there are three coexisting attracting cycles: γ_{14}, γ^1_{199} and γ^2_{199}, some points of which are shown together with their basins of attraction. Moreover, an attracting cycle may coexist with a chaotic attractor: see Fig. 15, which shows an attracting cycle γ_{14}, and a chaotic attractor together with their basins of attraction. An enlarged part of the chaotic attractor is shown in Fig. 16.

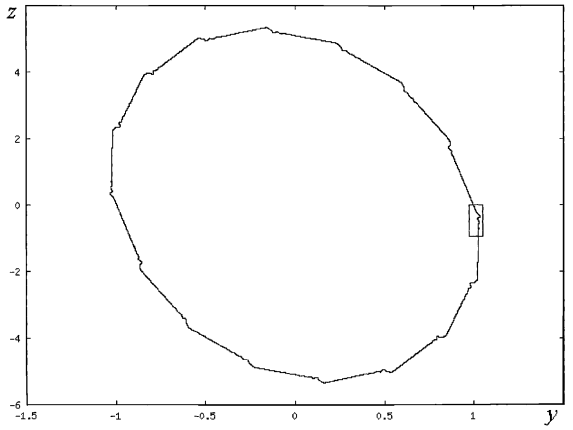

Fig. 12. Attracting closed invariant curve $\mathscr{A}$ of the map F at $v = 1.7$, $s = 0.84$ and $m = 0.075$. The portion in the rectangle is enlarged in Fig. 13.

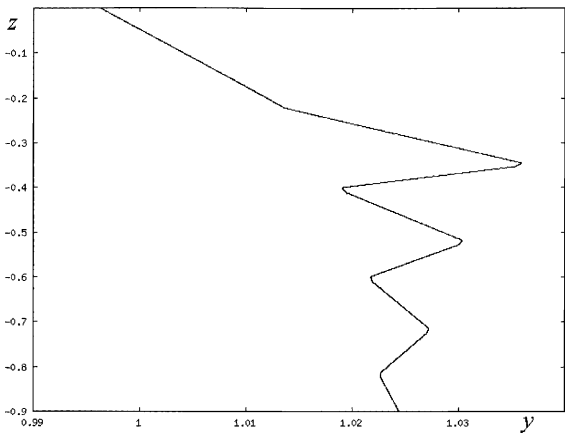

Fig. 13. An enlarged part of the curve $\mathscr{A}$ shown in Fig. 12.

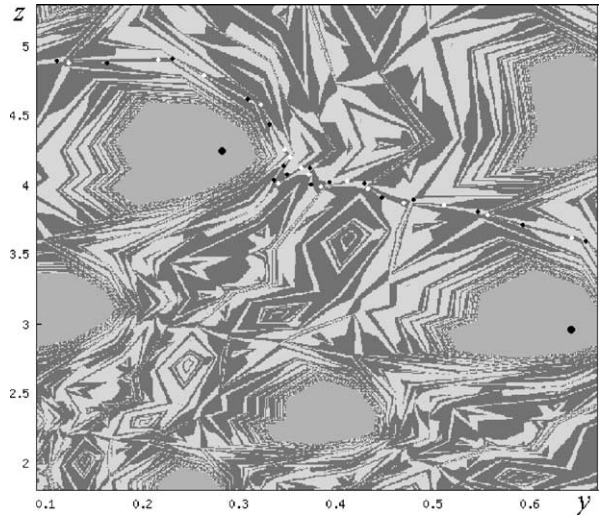

Fig. 14. Three coexisting attracting cycles γ_{14}, γ^1_{199} and γ^2_{199} of the map F, some points of which are shown together with their basins of attraction, at $v = 1.7$, $s = 0.8$ and $m = 0.1$.

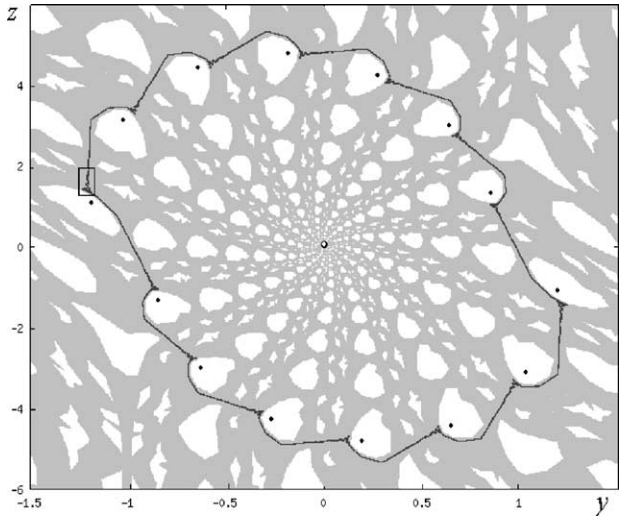

Fig. 15. Attracting cycle γ_{14} and a chaotic attractor together with their basins of attraction at $v = 1.7$, $s = 0.804$ and $m = 0.1$. The portion in the rectangle is enlarged in Fig. 16.

In order to see the shape of the resonance regions in the (s, v)-parameter plane, we present the corresponding two-dimensional bifurcation diagram for $m = 0.1$ (see Fig. 17). The feasible parameter range is indicated by the vertical lines $s = 0$ and $s = 0.9$. The k-resonance regions are denoted by the corresponding numbers $k \leqslant 34$. The white region, as before, represents either attracting cycles of periods $k > 34$, or quasi-periodic attractors, or chaos. From Fig. 17 we can see that in the feasible parameter range there are regions in which the map F is noninvertible ($s > 0.2$) and routes to complex dynamics with chaotic attractors can be realized. The sequence of bifurcations leading from an attracting cycle existing on the closed invariant curve $\mathscr{A}$ to a chaotic attractor, as the one shown in Fig. 15, is related to a homoclinic bifurcation of the saddle cycle belonging to $\mathscr{A}$, and to foldings and self-intersections of its unstable set (see [4,14]). We leave the detailed description of the destruction of the resonance regions for a future study.

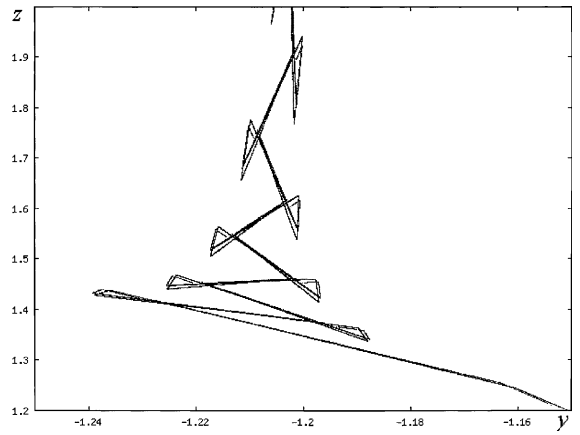

Fig. 16. An enlarged part of the chaotic attractor shown in Fig. 15.

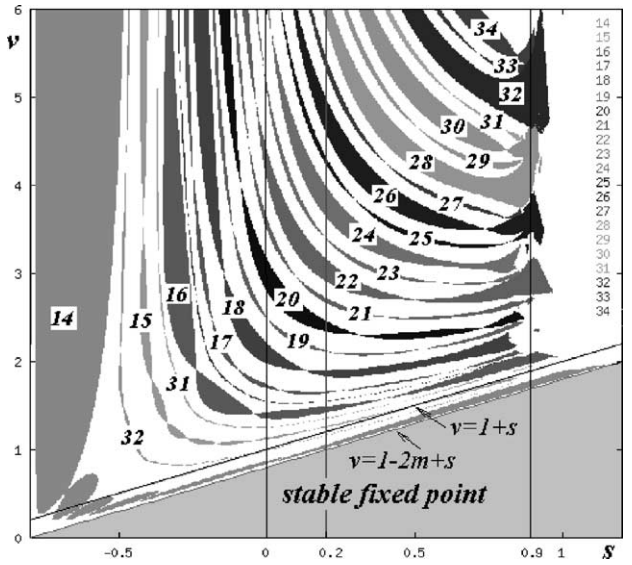

Fig. 17. Two-dimensional bifurcation diagram for the map F in the (s, v) parameter plane at $m = 0.1$.

4. The dynamics of the three-dimensional map T

In this section, we consider the three dimensional map T given in (10). In the previous section we have described the dynamics on the invariant plane $x = -y$. We are now interested in the asymptotic behaviour of the trajectories which do not belong to the T-invariant plane. Before considering the generic point let us first describe another particular set, the invariant line given by $\{x = y, z = 0\}$, on which the dynamics are defined by the one-dimensional map f of the form (14).

The map f has very simple dynamics: for $v < (s + 1)$ the origin is the only attracting fixed point. For $v > (s + 1)$ (see Fig. 18) the origin is repelling but there are two more fixed points: $p_0 = v/(1 + s)$ and $p_0' = -v/(1 + s)$. These fixed points attract all the points of the real axis except the preimages of the origin. In fact, the infinitely many preimages of $x = 0(\pm v/s, \pm v(1 + s)/s^2, \ldots)$ bound the intervals which belong, alternatively, to the basins of attraction of the fixed points p_0 and p_0', as shown in Fig. 18. At the bifurcation value $v = (s + 1)$, the map f has the segment $[-1,1]$ of fixed points (stable, but not attracting), and the trajectory of any other point of the real line finally ends up at one of these fixed points.

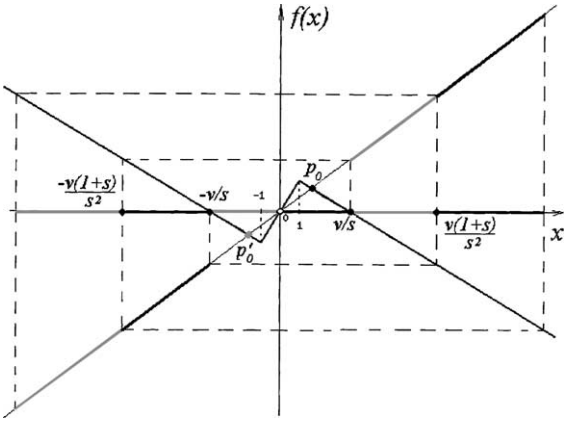

Fig. 18. One-dimensional map f to which the map T is reduced on the invariant line $\{x = y, z = 0\}$. Here $v > (s + 1)$.

Let us now turn to the global dynamics of the map T as given in (10).

Denote by R_i, $i = \overline{1,5}$ the following subregions of $\mathbb{R}^3$:

$$R_1 = \{(x,y,z) : x > 1, y < -1, z \in \mathbb{R}\},$$
$$R_2 = \{(x,y,z) : |x| \leqslant 1, |y| \leqslant 1, z \in \mathbb{R}\},$$
$$R_3 = \{(x,y,z) : x < -1, y > 1, z \in \mathbb{R}\},$$
$$R_4 = \{(x,y,z) : x < -1, y < -1, z \in \mathbb{R}\},$$
$$R_5 = \{(x,y,z) : x > 1, y > 1, z \in \mathbb{R}\}.$$

The point $(0,0,0) \in R_2$ obviously is a fixed point of the map T.

The eigenvalues of the map T in R_2 are $\lambda_{1,2}$ given in (16) (the corresponding eigenvectors belong to the invariant plane $x = -y$) and $\lambda_3 \stackrel{\text{def}}{=} \lambda_\perp = v - s$ (the corresponding eigenvector is transversal to the plane $x = -y$).

Proposition 8. *For $v < 1 + s$, the origin $(0,0,0)$ is the unique fixed point of the map T and it is globally attracting iff $(s,m) \in S$ where S is defined in* (15). *If $(s,m) \notin S$, $m < (1+s)/2$, then the origin is only transversally attracting.*

To show that this proposition is true, we first check that among the nine linear maps defining T, only one (the map in R_2) has the fixed point in its region of definition. Moreover, under the assumption of the proposition, all the linear maps have eigenvalues less than 1 in absolute value, i.e. all are contractions. Next, we note that $|\lambda_\perp| < 1$ if $v < 1 + s$. From Proposition 1, we have that $|\lambda_{1,2}| < 1$ if $(s,m) \in S$, and $|\lambda_{1,2}| > 1$ if $(s,m) \notin S$. Thus, the proposition is proved.

Let us now check when the invariant plane $x = -y$ is transversally attracting. The plane $x = -y$ belongs to the regions R_1, R_2 and R_3. We have shown that the map T in the region R_2 is transversally attracting if $v < 1 + s$. The eigenvalues of T in R_1 and R_3 are $\mu_{1,2}$ given in (17) and $\mu_3 \stackrel{\text{def}}{=} \mu_\perp = -s$, the same as for the maps in R_4 and R_5 (because the corresponding linear maps differ only by a shift constant). As $0 < s < 1$, we have $|\mu_\perp| < 1$. Thus, the following proposition holds

Proposition 9. *For $v < 1 + s$, the T-invariant plane $x = -y$ is globally attracting*; *The dynamics on it are described by the map F given in* (13).

Proposition 10. *If $v > 1 + s$ then, besides the attractors belonging to the invariant plane $x = -y$, the map T has two more fixed points $P_0 = (p_0, p_0, 0) \in R_5$ and $P_0' = (p_0', p_0', 0) \in R_4$, which are attracting iff $(s,m) \in S_1$, where S_1 is defined in* (18).

In fact, for $v > 1 + s$, besides the zero fixed point, the map T has two more fixed points $P_0 \in R_5$ and $P_0' \in R_4$. The eigenvalues of the map T in R_4 and R_5 are $\mu_{1,2}$ as given in (17) and $\mu_3 = -s$.

Let $\mathscr{B}(P_0)$ and $\mathscr{B}(P_0')$ denote the basins of attraction of the fixed points P_0 and P_0', respectively. These basins are volumes in $\mathbb{R}^3$. Figs. 19 and 20 show two-dimensional sections, $z = 0$ and $x = y$, respectively, of $\mathscr{B}(P_0)$ and $\mathscr{B}(P_0')$ at $s = 0.4$, $m = 0.5$, $v = 5$. The trajectories of initial points belonging to the white region are attracted to the period-6 cycle $\gamma_{1/6}$ existing on the invariant plane $x = -y$. The boundary of $\mathscr{B}(P_0)$ and $\mathscr{B}(P_0')$ is formed by polygons $\mathscr{P}_i$, $i = 1, 2, \ldots,$

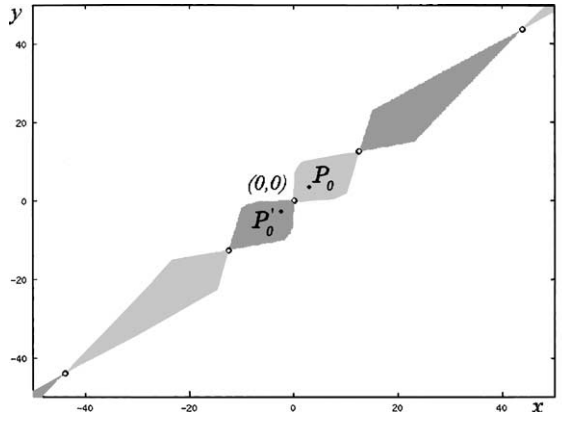

Fig. 19. Section $w = 0$ of the basins of attraction of the fixed points P_0 and P_0' at $s = 0.4$, $m = 0.5$ and $v = 5$.

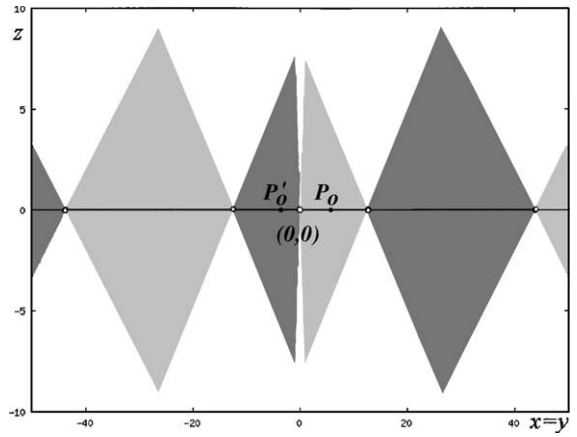

Fig. 20. Section $x = y$ of the basins of attraction of the fixed points P_0 and P_0' at $s = 0.4$, $m = 0.5$ and $v = 5$.

belonging to the preimages of the invariant plane $x = -y$. Section of $\mathscr{P}_i$ gives segments which form the boundary of $\mathscr{B}(P_0)$ and $\mathscr{B}(P_0')$ seen in Figs. 19 and 20, separated by the preimages of the origin.

5. Discussion

In the above analysis, we used the simplification that the locations of the "roof" and "ceiling" for the Hicks investment function were symmetric around the origin. For more generality we should skip this extreme assumption of symmetry. However, it can be shown that such an amendment would make but little difference as to the qualitative results obtained.

Further, recall that the reduction of the four dimensional map for the two region model to three dimensions was possible only due to the assumption of a special lag structure for consumption expenditures. Using in stead the original (simplest) lag structure, results in a non-reducible map in four dimensions, which itself deserves further study.

The same holds true for the original Hicks model for a single region (without interregional trade). Even if it cannot produce chaos, as mentioned above, it has interesting dynamic features not yet fully analysed.

Acknowledgements

The research is supported by the Landau Network/Cariplo Foundation, and by the Italian MURST via the National Research Group "Nonlinear Dynamics and Stochastic Models in Economics and Finance".

References

[1] Aronson DG, Chory MA, Hall GR, McGehee RP. Bifurcations from an invariant circle for two-parameter families of maps of the plane: a computer-assisted study. Commun Math Phys 1982;83:303–54.
[2] Boyland PL. Bifurcations of circle maps: Arnol'd tongues, bistability and rotation intervals. Commun Math Phys 1986;106:353–81.
[3] Frisch R. Propagation problems and impulse problems in dynamic economics. Economic essays in honour of Gustav Cassel. London: Alien & Unwin; 1933.
[4] Frouzakis CE, Gardini L, Kevrekidis I, Millerioux G, Mira C. On some properties of invariant sets of two-dimensional noninvertible maps. Int J Bifur Chaos 1997;7(6):1167–94.
[5] Goodwin RM. The nonlinear accelerator and the persistence of business cycles. Econometrica 1951;19:1–17.
[6] Guckenheimer J, Holmes JP. Nonlinear oscillations, dynamical systems, and bifurcations of vector fields. Berlin: Springer-Verlag; 1983.
[7] Gumovski I, Mira C. Recurrences and discrete dynamical systems. Berlin: Springer-Verlag; 1980.
[8] Harrod RF. Towards a dynamic economics. London: Macmillan; 1948.
[9] Hicks JR. A contribution to the theory of the trade cycle. Oxford: Oxford University Press; 1950.
[10] Hommes CH. Chaotic dynamics in economic models. Groningen: Wolters-Noodhoff; 1991.
[11] Kuznetsov Y. Elements of applied bifurcation theory. Berlin: Springer-Verlag; 1995.
[12] Maistrenko Y, Sushko I, Gardini L. About two mechanisms of reunion of chaotic attractors. Chaos, Solitons & Fractals 1998;9(8):1373–90.
[13] Metzler LA. A multiple-region theory of income and trade. Econometrica 1950;18:329–54.
[14] Mira C, Gardini L, Barugola A, Cathala JC. Chaotic dynamics in two-dimensional noninvertible maps. Singapore: World Scientific; 1996.
[15] Nusse HE, Yorke JA. Border-collision bifurcations including ''period two to period three'' for piecewise smooth systems. Phys D 1992;57:39–57.
[16] Phillips AW. Stabilization policy in a closed economy. Econ J 1954;64:290–323.
[17] Puu T. Nonlinear economic dynamics. In: Lecture notes in economics and mathematical systems, vol. 336. Berlin: Springer; 1989.
[18] Samuelson PA. Interactions between the multiplier analysis and the principle of acceleration. Rev Econ Stat 1939;21:75–8.